

Received:
22 December 2014

Revised:
10 July 2015

Accepted:
20 July 2015

doi: 10.1259/bjr.20140863

Cite this article as:

Bangiyev L, Raz E, Block TK, Hagiwara M, Wu X, Yu E, et al. Evaluation of the orbit using contrast-enhanced radial 3D fat-suppressed T_1 weighted gradient echo (Radial-VIBE) sequence. *Br J Radiol* 2015; **88**: 20140863.

FULL PAPER

Evaluation of the orbit using contrast-enhanced radial 3D fat-suppressed T_1 weighted gradient echo (Radial-VIBE) sequence

¹LEV BANGIYEV, DO, ²EYTAN RAZ, MD, ²TOBIAS K BLOCK, PHD, ²MARI HAGIWARA, MD, ²XIN WU, MD, ³EUGENE YU, MD and ²GIRISH M FATTERPEKAR, MD

¹Department of Radiology, Stony Brook University Medical Center, Stony Brook, NY, USA

²Department of Radiology, NYU Langone Medical Center, New York, NY, USA

³Department of Radiology, University of Toronto, Toronto, ON, Canada

Address correspondence to: Lev Bangiyev

E-mail: Lev.Bangiyev@stonybrookmedicine.edu

Paper presented at ASNR 2013 meeting in San Diego, CA, USA.

Objective: Contrast-enhanced fat-suppressed T_1 weighted (T1W) two-dimensional (2D) turbo spin echo (TSE) and magnetization-prepared gradient echo (MPRAGE) sequences with water excitation are routinely obtained to evaluate orbit pathology. However, these sequences can be marred by artefacts. The radial-volume-interpolated breath-hold examination (VIBE) sequence is a motion-robust fat-suppressed T1W sequence which has demonstrated value in paediatric and body imaging. The purpose of our study was to evaluate its role in assessing the orbit and to compare it with routinely acquired sequences.

Methods: A Health Insurance Portability and Accountability Act-compliant and institutional review board-approved retrospective study was performed in 46 patients (age range: 1-81 years) who underwent orbit studies on a 1.5-T MRI system using contrast-enhanced Radial-VIBE, MPRAGE and 2D TSE sequences. Two radiologists blinded to the sequence analysed evaluated multiple parameters of image quality including motion artefact, degree of fat suppression, clarity of choroidal enhancement, intra-orbital vessels, extraocular muscles, optic nerves, brain

parenchyma and evaluation of pathology. Each parameter was assessed on a 5-point scale, with a higher score indicating the more optimal examination. Mix model analysis of variance and interobserver variability were assessed.

Results: Radial-VIBE demonstrated superior quality ($p < 0.001$) for all orbit parameters when compared with MPRAGE and 2D TSE. Interobserver agreement demonstrated average fair-to-good agreement for degree of motion artefact (0.745), fat suppression (0.678), clarity of choroidal enhancement (0.688), vessels (0.655), extraocular muscles (0.675), optic nerves (0.518), brain parenchyma (0.710) and evaluation of pathology (0.590).

Conclusion: Radial-VIBE sequence demonstrates superior image quality when evaluating the orbits as compared with conventional MPRAGE and 2D TSE sequences.

Advances in knowledge: Radial-VIBE employs unique non-Cartesian k-space sampling in a radial or spoke-wheel fashion which provides superior image quality improving diagnostic capability in the evaluation of the orbits.

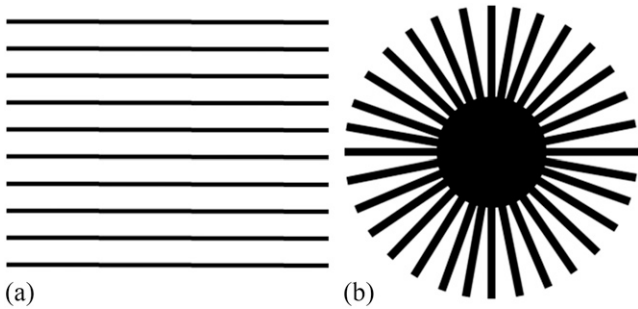
INTRODUCTION

Traditionally, contrast-enhanced T_1 weighted (T1W) fat-suppressed two-dimensional (2D) turbo spin echo (TSE) sequence and three-dimensional (3D) magnetization-prepared gradient echo (MPRAGE) sequence with water excitation (WE) are used to evaluate the orbits. However, they are susceptible to eyelid or globe motion-related artefacts and inhomogeneous fat saturation.^{1,2}

In both these sequences, k-space sampling is performed using a conventional Cartesian scheme, also known as

phase-encoding scheme, which acquires the data in a row-by-row fashion (Figure 1a). Radial-volume-interpolated breath-hold examination (VIBE) is a T1W radial 3D gradient echo sequence which uses a non-Cartesian approach by sampling k-space in a radial, spoke-wheel fashion in the X-Y plane (Figure 1b) and with normal Cartesian sampling in the Z-dimension, which results in a "stack-of-stars" trajectory in k-space^{3,4} (Figure 2). This unique k-space sampling scheme provides significant reduction in motion artefact. In addition, Radial-VIBE achieves a homogeneous degree of fat suppression. These factors have seen Radial-VIBE

Figure 1. A schematic representation of conventional Cartesian row-by-row k-space sampling (a) and radial or spoke-wheel sampling (b) used in radial-volume-interpolated breath-hold examination (Radial-VIBE).



being routinely used in body and paediatric imaging.⁵⁻⁷ However, evaluation of the orbit using Radial-VIBE has not been studied. The purpose of our study was to determine the role of contrast-enhanced Radial-VIBE in assessing the orbits and compare it with currently accepted clinical standard of care, including contrast-enhanced T1W MPRAGE WE and fat-suppressed 2D TSE images.

Figure 2. In radial-volume-interpolated breath-hold examination (Radial-VIBE), spoke-wheel k-space sampling occurs in the X-Y plane with traditional Cartesian sampling in the Z-dimension resulting in a “stack-of-stars” trajectory.

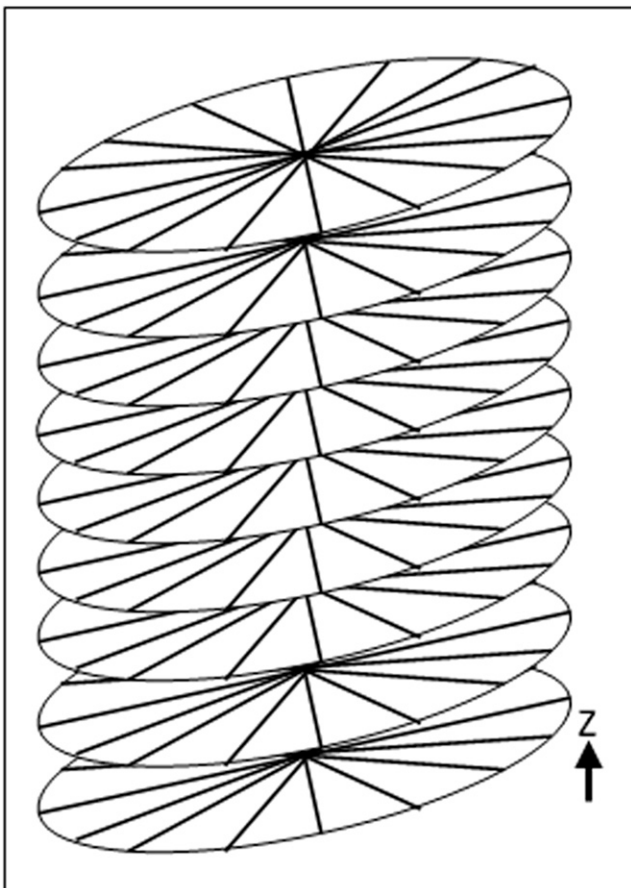


Table 1. Image quality scores for each reader and each sequence (mean ± standard deviation)

Sequence/parameter	Radial-VIBE		Ax magnetization-prepared gradient echo		Ax FS T1W		Cor FS T1W		Cor Radial-VIBE	
	Reader 1	Reader 2	Reader 1	Reader 2	Reader 1	Reader 2	Reader 1	Reader 2	Reader 1	Reader 2
	Motion artefact	5.00 ± 0	4.91 ± 0.29	3.98 ± 0.65	3.72 ± 0.72	4.07 ± 0.73	3.93 ± 0.62	4.59 ± 0.56	4.31 ± 0.54	5.0 ± 0
Degree of fat suppression	4.65 ± 0.8	4.63 ± 0.71	3.8 ± 1.00	3.59 ± 0.78	3.29 ± 0.91	3.5 ± 1.02	3.81 ± 0.64	3.81 ± 0.59	4.78 ± 0.42	4.78 ± 0.49
Clarity of chorioidal enhancement	5.00 ± 0	4.96 ± 0.21	4.76 ± 0.43	4.3 ± 0.7	4.14 ± 0.86	4.0 ± 0.78	3.72 ± 0.52	3.94 ± 0.76	5.0 ± 0	4.97 ± 0.18
Clarity of the vessel	4.89 ± 0.32	4.93 ± 0.25	3.52 ± 0.66	3.83 ± 0.61	2.79 ± 0.43	3.14 ± 0.66	3.0 ± 0.36	3.41 ± 0.71	4.84 ± 0.37	4.97 ± 0.18
Clarity of the muscle	4.98 ± 0.15	4.89 ± 0.32	4.22 ± 0.79	4.13 ± 0.78	4.57 ± 0.51	4.07 ± 0.73	4.44 ± 0.67	4.22 ± 0.49	5.0 ± 0	4.94 ± 0.25
Clarity of optic nerve	5.00 ± 0	4.85 ± 0.36	3.76 ± 0.9	3.7 ± 0.84	2.64 ± 0.63	3.36 ± 0.75	3.38 ± 0.71	3.53 ± 0.67	5.0 ± 0	4.91 ± 0.3
Clarity of brain parenchyma	4.67 ± 0.47	4.33 ± 0.52	4.87 ± 0.34	4.35 ± 0.6	2.21 ± 0.58	2.29 ± 0.47	2.16 ± 0.37	2.38 ± 0.49	4.72 ± 0.46	4.5 ± 0.57
Conspicuity of pathology	4.71 ± 0.85	4.74 ± 0.53	3.96 ± 1.07	3.86 ± 0.89	3.6 ± 1.08	3.4 ± 0.7	3.22 ± 1.17	3.67 ± 0.77	4.67 ± 0.97	4.61 ± 0.98

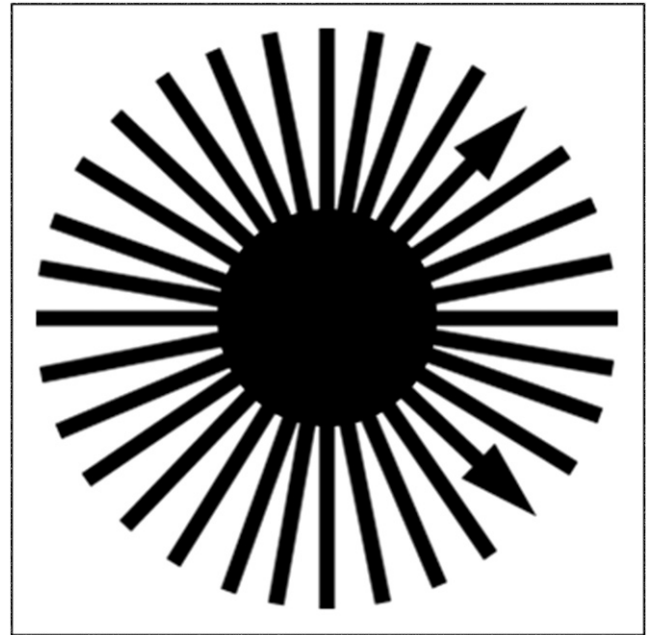
Ax, axial; Cor, coronal; FS, fat saturated; T1W, T₁ weighted; VIBE, volume-interpolated breath-hold examination.

Table 2. Image quality scores averaged over two readers (mean ± standard deviation) with *p*-values and interobserver agreement

Parameter/sequence	Volume-interpolated breath-hold examination	Three-dimensional multiplanar reconstructions	T1FScore	T1FSax	VIBEScore	<i>p</i> -value	Agreement
Motion artefacts	4.96 ± 0.21	3.85 ± 0.69	4.45 ± 0.56	4.00 ± 0.67	4.98 ± 0.13	<0.001	0.74
Fat suppression	4.64 ± 0.75	3.70 ± 0.90	3.81 ± 0.61	3.39 ± 0.96	4.78 ± 0.45	<0.001	0.68
Clarity of scleral enhancement	4.98 ± 0.15	4.53 ± 0.62	3.83 ± 0.66	4.07 ± 0.81	4.98 ± 0.13	<0.001	0.69
Orbital vessels definition	4.91 ± 0.28	3.67 ± 0.65	3.20 ± 0.60	2.96 ± 0.58	4.91 ± 0.29	<0.001	0.66
Orbital muscles definition	4.93 ± 0.25	4.17 ± 0.78	4.33 ± 0.59	4.32 ± 0.67	4.97 ± 0.18	<0.001	0.67
Nerve sheath complex	4.92 ± 0.27	3.73 ± 0.87	3.45 ± 0.69	3.00 ± 0.77	4.95 ± 0.21	<0.001	0.52
Overall brain parenchyma appearance	4.50 ± 0.52	4.61 ± 0.55	2.27 ± 0.45	2.25 ± 0.52	4.61 ± 0.52	<0.001	0.71
Pathology conspicuity	4.73 ± 0.71	3.91 ± 0.98	3.44 ± 1.00	3.50 ± 0.89	4.64 ± 0.96	<0.001	0.59

T1FSax, T1 weighted fat saturated axial; T1FScore, T1 weighted fat saturated coronal; VIBEScore, radial-volume-interpolated breath-hold examination coronal.

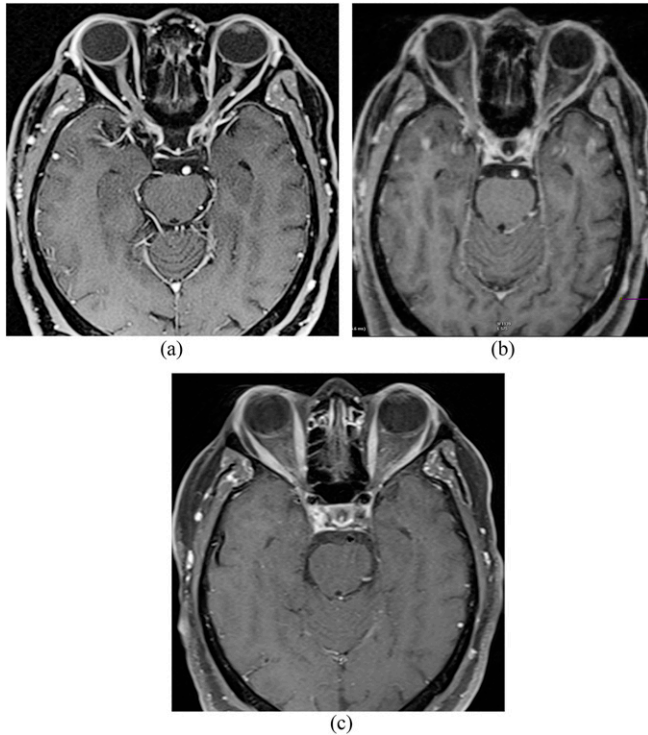
Figure 3. Each k-space line in radial-volume-interpolated breath-hold examination (Radial-VIBE) is acquired with a different readout direction.



METHODS AND MATERIALS

A Health Insurance Portability and Accountability Act-compliant retrospective study was performed after approval of the institutional review board. The study included 46 patients (age range: 1–81 years) who underwent clinically indicated contrast-enhanced MRI of the orbits on a 1.5-T system (MAGNETOM® Avanto; Siemens Healthcare, Erlangen, Germany) using a 12-channel head coil. In addition to the standard non-contrast sequences, the patients were evaluated with Radial-VIBE as well as conventional T1W MPRAGE WE and fat-suppressed 2D TSE sequences. Radial-VIBE was performed after the administration of 0.01 mmol kg⁻¹ of gadolinium-based contrast at 3 ml s⁻¹, followed by the conventional sequences. The following imaging parameters were used for Radial-VIBE: spatial resolution 0.8 × 0.8 × 0.8 mm, field of view (FOV) 250 mm², 96 slices, repetition time (TR) 4.57 ms, echo time (TE) 2.06 ms, flip angle 12°, matrix 288 × 288, 800 radial spokes, bandwidth (BW) 400 Hz per pixel, acquisition time 4 : 43 min. The MPRAGE WE sequence was obtained with the following imaging parameters: spatial resolution 1.0 × 1.0 × 1.0 mm, FOV 250 mm², 160 slices (to include entire brain parenchyma as per the standard protocol), TR 2150 ms, TE 5.57 ms, flip angle 15°, matrix 256 × 187, BW 349 Hz per pixel, acquisition time 4 : 01 min. Of note, reducing the number of slices would not lead to shorter acquisition time, which is constrained by the needed magnetization-preparation delay for the MPRAGE sequence. Fat-saturated T1W 2D TSE sequence was obtained in the axial plane with the following imaging parameters: spatial resolution 0.63 × 0.63 × 4.0 mm, FOV 250 mm², 20 slices, TR 444 ms, TE 13 ms, flip angle 90°/180°, matrix 256 × 192, BW 161 Hz per pixel, acquisition time 4 : 27 min (axial). The clinical protocol also included a 2D TSE scan in coronal orientation with an acquisition time of 3 : 49 min.

Figure 4. (a) Radial-volume-interpolated breath-hold examination (Radial-VIBE), (b) three-dimensional magnetization-prepared gradient echo and (c) T_1 turbo spin echo with fat suppression MRI sequences with contrast demonstrate superior image quality of Radial-VIBE in terms of motion, clarity of the optic nerve, choroidal enhancement, clarity of the extraocular muscles, fat suppression and clarity of intraorbital vessels.



Imaging evaluation

Two neuroradiologists, GMF with 15 years' experience and ER with 5 years' experience, independently evaluated the studies. Both readers were blinded to the sequences analysed. Image quality was assessed by evaluating the degree of motion artefact, quality of fat suppression, clarity of choroidal enhancement, vessels, extraocular muscles, optic nerve, brain parenchyma and conspicuity of pathology. Each parameter was graded on a five-point scale: 5 excellent, 4 good, 3 acceptable, 2 poor and 1 unacceptable.

Statistical analysis

Statistical analysis was performed using SPSS® (released 2012, IBM SPSS Statistics for Windows, v. 21.0; IBM Corporation, Armonk, NY). The data are expressed as mean values with \pm standard deviation. Kruskal–Wallis test was used to compare the result of axial Radial-VIBE, axial MPRAGE WE and axial T_1 fat-saturated sequences. A Mann–Whitney U test was performed to compare the grading of the contrast-enhanced coronal reconstructed Radial-VIBE with that of conventional fat-suppressed coronal T1W sequence. Using Cohen's kappa analysis, an interobserver agreement assessment was also performed.

RESULTS

The individual reader grades for each parameter are listed in Table 1. The average grades and interobserver variability are

shown in Table 2. The grades assessed for each individual parameter, including motion artefact, degree of fat suppression, clarity of choroidal enhancement, vessels, extraocular muscles, optic nerve and conspicuity of pathology, were significantly higher ($p < 0.001$) for all the parameters of the axial Radial-VIBE sequence than for MPRAGE WE and fat-suppressed 2D TSE. Evaluation of brain parenchyma was slightly better on the MPRAGE WE sequence than on the Radial-VIBE. The interobserver agreement in the qualitative evaluation using a Cohen's kappa analysis demonstrated average fair-to-good agreement for the following variables: motion artefact (0.745), degree of fat suppression (0.678), clarity of choroidal enhancement (0.688), vessels (0.655), extraocular muscles (0.675), optic nerve (0.518), brain parenchyma (0.710) and conspicuity of pathology (0.590).

DISCUSSION

This study demonstrates superior image quality of Radial-VIBE in comparison with traditional 3D MPRAGE WE and fat-suppressed 2D TSE sequences in terms of motion robustness, fat suppression, anatomic clarity and conspicuity of orbit pathology.

Motion artefacts have always been a limitation in MRI owing to the pronounced sensitivity of conventional "phase-encoded" sequences. In MRI sequences that employ conventional Cartesian k-space sampling, motion effects such as patient movement or blood flow lead to phase offsets of the signal as a result of the Fourier shift property and disturb the constant phase difference

Figure 5. (a) Axial and (b) coronal radial-volume-interpolated breath-hold examination (Radial-VIBE) with contrast demonstrate sharper delineation of intraorbital meningioma in comparison with conventional sequences. (c) Axial three-dimensional magnetization-prepared gradient echo with contrast and (d) contrast-enhanced coronal T_1 turbo spin echo with fat suppression.

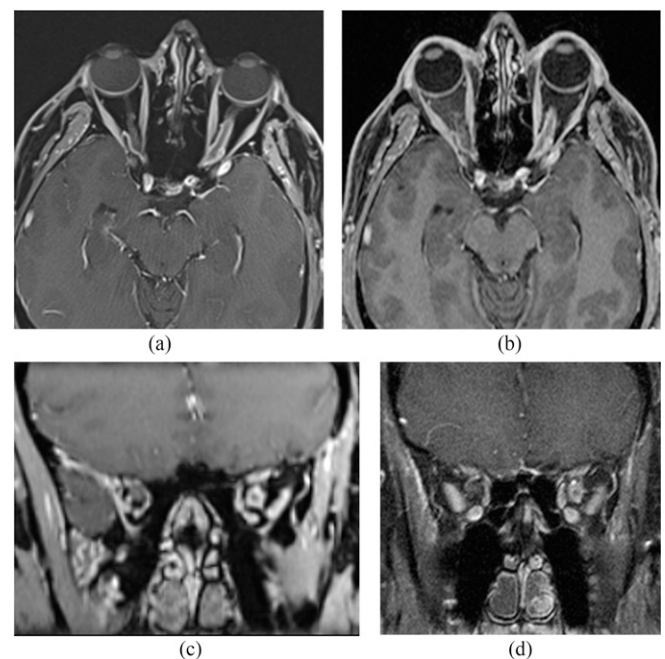
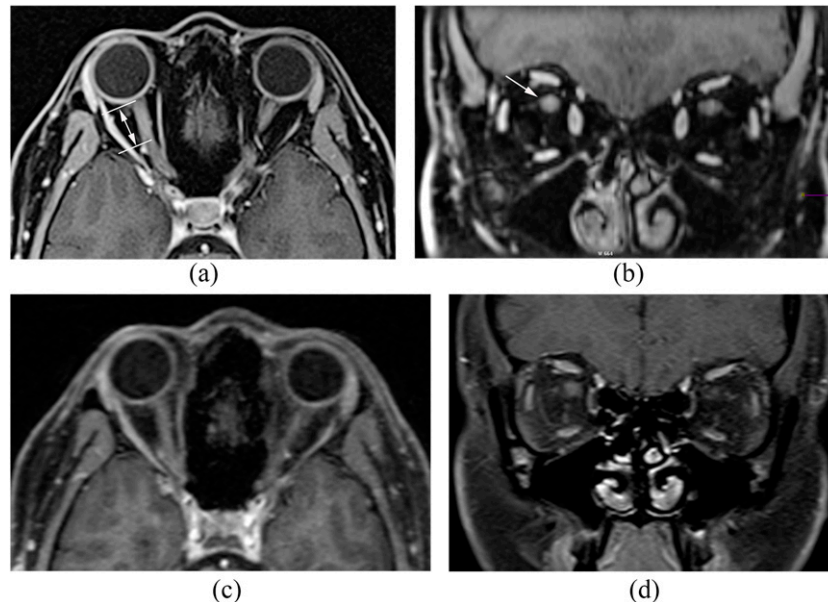


Figure 6. Post-contrast (a) axial and (b) coronal radial-volume-interpolated breath-hold examination (Radial-VIBE) images demonstrate relatively sharply defined segmental enhancement (double headed arrow) of the intraorbital portion of the right optic nerve (arrow) consistent with suspected optic neuritis. In comparison, (c) post-contrast axial three-dimensional magnetization-prepared gradient echo with water excitation and (d) post-contrast coronal two-dimensional T_1 turbo spin echo with fat suppression images demonstrate subtle asymmetric enhancement of the right optic nerve.



between sampled k-space rows. This can be interpreted as displacing individual lines along the phase-encoding direction, which results in the appearance of dominant aliasing effects, known as “ghosting” artefacts. Recently, MRI techniques known as PROPELLER or BLADE have been introduced to address the motion-artefact problem, which acquire k-space data using “blades” consisting of multiple parallel lines that are rotated in k-space in a radial-type scheme.^{8–11} These techniques have demonstrated the substantial improvement in image quality for T_2 weighted 2D TSE acquisitions as well as diffusion-weighted imaging sequences. However, the significant overlap of the blades in k-space leads to inefficient k-space acquisition and, thus, to long acquisition times, which make it impractical to use these sequences for many clinical applications. Radial-VIBE uses a similar concept, but here, only a single line is rotated in k-space instead of a wide blade, leading to higher scan efficiency and making the sequence competitive to other T1W sequences. Because a phase-encoding direction does not exist in the radial sampling scheme, and each k-space line is acquired with a different readout direction, as illustrated in Figure 3, motion-induced phase distortions cannot lead to appearance of aliasing effects. Furthermore, the overlap of the radial spokes in the k-space centre has a time-averaging effect that additionally reduces the sensitivity to motion. While Radial-VIBE examinations are generally free of ghosting artefacts, motion can still translate into radially oriented streaks or mild blurring.⁶ However, in our study, we encountered minimal if any noticeable such streak artefact or blurring, without appreciable image-quality degradation.

Inadvertent globe or eyelid motion often degrades the quality of conventional 3D MPRAGE WE and fat-suppressed 2D TSE examinations, which limits the evaluation of orbit and its anatomic contents. Furthermore, the relatively abundant amount of

retrobulbar fat is not always homogeneously suppressed on conventional fat-saturated sequences. Involuntary motion and inadequate fat suppression remain the primary two limitations when evaluating the orbit. Our study clearly demonstrates that Radial-VIBE, owing to its more uniform fat suppression and advantageous k-space sampling, provides adequate motion robustness and allows for a more optimal evaluation of orbital contents, such as the sclera, extraocular muscles, optic nerves, vessels and underlying intraorbital pathology (Figure 4).

Moreover, improved in-plane resolution is achieved with the Radial-VIBE sequence (0.8×0.8 mm) in comparison with the 3D MPRAGE WE protocol (1.0×1.0 mm). The 2D TSE protocol has superior in-plane resolution (0.63×0.63 mm) but uses a large slice thickness of 4 mm, which makes it impossible to reconstruct these images in different orientations and, thus, requires separate acquisitions for each orientation. Because Radial-VIBE data are acquired in an isotropic manner at 0.8 mm spatial resolution, multiplanar reconstructions (MPR) can be created without compromise in image quality.

The abovementioned improved image qualities provide for superior depiction and characterization of lesions in the orbits. Representative illustrations include intraorbital meningioma (Figure 5) and optic neuritis (Figure 6). In each of these cases, Radial-VIBE demonstrates artefact-free and a more crisp depiction of intraorbital pathology.

The acquisition time for the Radial-VIBE protocol (4:43 min) is slightly longer than that of the MPRAGE WE (4:01 min) and fat-suppressed 2D TSE (4:27 min) protocols. However, due to the MPR capability of the Radial-VIBE sequence, a single acquisition

is sufficient for evaluating the orbits in different orientations, which results in overall shorter examination time.

In conclusion, our study has demonstrated superior image quality of Radial-VIBE in comparison with conventional MPRAGE

and 2D TSE sequences and should be used routinely as part of standard orbit MRI protocol.

FUNDING

This work was supported by NYU Langone Medical Center.

REFERENCES

1. Axel L, Summers RM, Kressel HY, Charles C. Respiratory effects in two-dimensional Fourier transform MR imaging. *Radiology* 1986; **160**: 795–801. doi: [10.1148/radiology.160.3.3737920](https://doi.org/10.1148/radiology.160.3.3737920)
2. Barakos JA, Dillon WP, Chew WM. Orbit, skull base, and pharynx: contrast-enhanced fat suppression MR imaging. *Radiology* 1991; **179**: 191–8. doi: [10.1148/radiology.179.1.2006277](https://doi.org/10.1148/radiology.179.1.2006277)
3. Song HK, Dougherty L. Dynamic MRI with projection reconstruction and KWIC processing for simultaneous high spatial and temporal resolution. *Magn Reson Med* 2004; **52**: 815–24. doi: [10.1002/mrm.20237](https://doi.org/10.1002/mrm.20237)
4. Lin W, Guo J, Rosen MA, Song HK. Respiratory motion-compensated radial dynamic contrast-enhanced (DCE)-MRI of chest and abdominal lesions. *Magn Reson Med* 2008; **60**: 1135–46. doi: [10.1002/mrm.21740](https://doi.org/10.1002/mrm.21740)
5. Azevedo RM, de Campos RO, Ramalho M, Herédia V, Dale BM, Semelka RC. Free-breathing 3D T1-weighted gradient-echo sequence with radial data sampling in abdominal MRI: preliminary observations. *AJR Am J Roentgenol* 2011; **197**: 650–7. doi: [10.2214/AJR.10.5881](https://doi.org/10.2214/AJR.10.5881)
6. Chandarana H, Block TK, Rosenkrantz AB, Lim RP, Kim D, Mossa DJ, et al. Free-breathing radial 3D fat-suppressed T1-weighted gradient echo sequence: a viable alternative for contrast-enhanced liver imaging in patients unable to suspend respiration. *Invest Radiol* 2011; **46**: 648–53. doi: [10.1097/RLI.0b013e31821eea45](https://doi.org/10.1097/RLI.0b013e31821eea45)
7. Chandarana H, Block KT, Winfeld MJ, Lala SV, Mazori D, Giuffrida E, et al. Free-breathing contrast-enhanced T1-weighted gradient-echo imaging with radial k-space sampling for paediatric abdominopelvic MRI. *Eur Radiol* 2013; **24**: 320–6. doi: [10.1007/s00330-013-3026-4](https://doi.org/10.1007/s00330-013-3026-4)
8. Deng J, Miller FH, Salem R, Omary RA, Larson AC. Multishot diffusion-weighted PROPELLER magnetic resonance imaging of the abdomen. *Invest Radiol* 2006; **41**: 769–75. doi: [10.1097/01.rli.0000236808.84746.95](https://doi.org/10.1097/01.rli.0000236808.84746.95)
9. Hirokawa Y, Isoda H, Maetani YS, Arizono S, Shimada K, Togashi K. Evaluation of motion correction effect and image quality with the periodically rotated overlapping parallel lines with enhanced reconstruction (PROPELLER) (BLADE) and parallel imaging acquisition technique in the upper abdomen. *J Magn Reson Imaging* 2008; **28**: 957–62. doi: [10.1002/jmri.21538](https://doi.org/10.1002/jmri.21538)
10. Deng J, Omary RA, Larson AC. Multishot diffusion-weighted SPLICE PROPELLER MRI of the abdomen. *Magn Reson Med* 2008; **59**: 947–53. doi: [10.1002/mrm.21525](https://doi.org/10.1002/mrm.21525)
11. Hirokawa Y, Isoda H, Maetani YS, Arizono S, Shimada K, Togashi K. MRI artifact reduction and quality improvement in the upper abdomen with PROPELLER and prospective acquisition correction (PACE) technique. *AJR Am J Roentgenol* 2008; **191**: 1154–8. doi: [10.2214/AJR.07.3657](https://doi.org/10.2214/AJR.07.3657)